

Low-Noise Cooled GASFET Amplifiers

SANDER WEINREB, FELLOW, IEEE

Abstract—Measurements of the noise characteristics of a variety of gallium-arsenide field-effect transistors at a frequency of 5 GHz and temperatures of 300 K to 20 K are presented. For one transistor type detailed measurements of dc parameters, small-signal parameters, and all noise parameters (T_{\min} , R_{opt} , X_{opt} , g_n) are made over this temperature range. The results are compared with the theory of Pucel, Haus, and Stutz modified to include the temperature variation. Several low-noise amplifiers are described including one with a noise temperature of 20 K over a 500-MHz bandwidth. A theoretical analysis of the thermal conduction at cryogenic temperatures in a typical packaged transistor is included.

I. INTRODUCTION

THE PRESENT state of the art for microwave low-noise amplifiers is shown in Fig. 1. The gallium-arsenide field-effect transistor (GASFET) amplifier does not yet achieve the noise temperature of the very best parametric amplifiers but is equal to or better than many paramps manufactured 10 years ago. In addition, the GASFET has higher stability and lower cost because of two inherent advantages: 1) it is much less critical to circuit impedance than a negative resistance amplifier such as a paramp; 2) it is powered by dc whereas the paramp requires a power oscillator and tuned circuits at several times the frequency of operation.

There are systems, particularly those requiring large-area antennas such as radio astronomy or space communications, where no present device operating at room temperature has sufficiently low noise. This is shown clearly in Fig. 1 where, in the 0.5–20-GHz range, the 300 K paramp performance is typically an order of magnitude greater than the natural noise limits of galactic, cosmic, and atmospheric noise. The lowest noise, highest cost solution is a maser or parametric up-converter-into-maser system operating at 4 K. Intermediate in cost and performance are paramps and GASFET's cooled to 20 K by closed-cycle helium refrigerators which are now available [10] at a cost of under \$5000 and a weight less than 45 kg.

Several reports of the noise temperature of cryogenically cooled GASFET amplifiers have been made [4]–[8] but, for the most part, these are for one specific device, do not determine the four noise parameters which characterize the noise of a linear two-port ([4] is an exception to this), do not report the device dc and small-signal parameters as a function of temperature, and do not attempt to correlate the results with theory. An attempt will be made to do the above in this paper and to present some information regarding the following questions.

Manuscript received April 3, 1980; revised June 24, 1980. The National Radio Astronomy Observatory is operated by Associated Universities, Inc., under contract to the National Science Foundation.

The author is with National Radio Astronomy Observatory, Charlottesville, VA 22903.

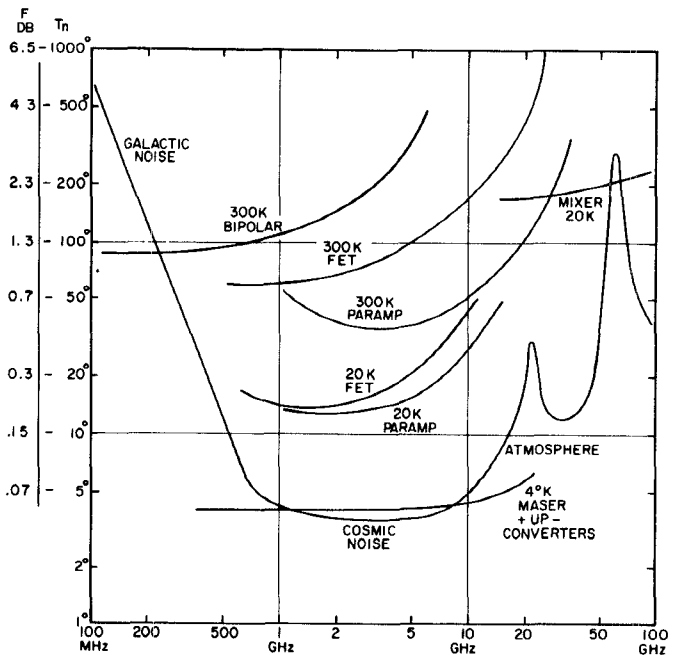


Fig. 1. Noise figure $10 \log F$, and noise temperature $T_n = 290^\circ$ ($F - 1$), versus frequency for various 1980 state-of-the-art low-noise devices. The 300 K bipolar transistor, FET, and paramp values are taken from manufacturers data sheets [1]–[3], the 20 K FET curve is from the data of this paper plus data of others [4]–[6] at 0.6, 1.4, and 12 GHz, respectively. The 20 K paramp, 4 K maser (including parametric up-converter at lower frequencies), and 20 K mixer results (which are SSB and include IF noise) are from systems in use at National Radio Astronomy Observatory (NRAO). The natural noise limitations due to galactic noise, the cosmic background radiation, and atmospheric noise are for optimum conditions and are taken from [9] plus points at 22 GHz and 100 GHz measured at NRAO.

- 1) Considering the dc power dissipated and thermal resistance problems, what is the actual physical temperature of the FET channel? What is the lowest physical temperature which can be achieved in the channel?
- 2) What is the noise improvement factor for cooling of presently available low-noise GASFET's? Are one manufacturer's devices superior for some fortuitous reason?
- 3) Can the present room-temperature GASFET noise theory be applied at cryogenic temperatures?
- 4) Can a GASFET be specifically designed for the best performance at cryogenic temperatures?
- 5) Is there any difference in the circuit design for a cryogenic amplifier?

II. THERMAL RESISTANCE

The room-temperature thermal resistance of a typical low-noise GASFET is specified on manufacturers' data sheets and is of the order of 100 K/W for a chip and 200

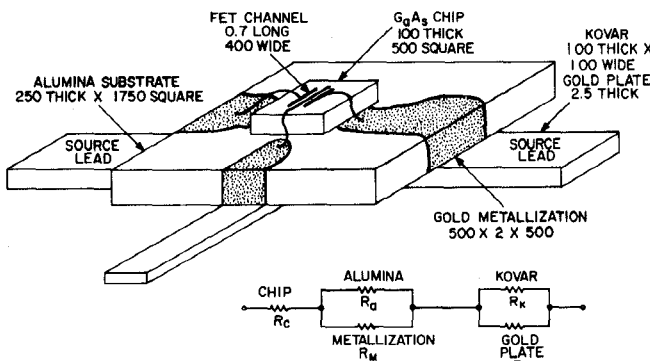


Fig. 2. Typical GASFET chip in 1.75-mm² package with top cover removed; all dimensions are in micrometers. Heat flow is from the FET channel spreading through the GaAs chip into the gold-metallized alumina substrate and out the source leads. An equivalent electrical circuit is also shown with thermal resistance values in Table I. Some manufacturers do not connect the source metallization to the chip.

TABLE I
THERMAL RESISTANCE OF PACKAGED GASFET IN K/W AND IN
PARENTHESIS MATERIAL CONDUCTIVITIES
IN W/K·cm

Component (Dimensions in μm)	R	Temperature			
		300°	77°	20°	4°
FET Channel (0.7 x 400)	R_c (0.44)	120 (4.4)	12 (4.4)	13 (4.1)	840 (.06)
Alumina Substrate 250 x (1.750) ²	R_a (0.35)	55 (1.5)	13 (1.5)	85 (0.23)	3900 (.005)
Gold Metallization 500 x (500 x 5)	R_m	335 (3)	285 (3.5)	62 (16)	45 (22)
Total $R_c + R_a // R_m$	R_t	169	24	49	885
Kovar in Source Leads 250 x (100 x 1000)	R_k (.165)	76 (.08)	156 (.08)	625 (.02)	4170 (.003)
Gold Plate on Source Leads 250 x 2.5 x 2200	R_p (3)	76 (3)	65 (3.5)	14 (16)	10 (22)
Total Including Source Leads $R_t + R_k // R_p$	R_T	207	89	63	895
Add for Epoxy Bond of Chip 25 x (500 x 500)	- (.02)	50 EST	100 (.01)	330 (.003)	1000 EST (.001)

K/W for a packaged device. These values produce a heating of 5 or 10 K for a typical low-noise dc power dissipation of 50 mW and do not significantly effect the room-temperature performance. However, at cryogenic temperatures the situation may be drastically different because the thermal conductivity of most materials changes by orders of magnitude; pure metals and crystalline substances become better thermal conductors while alloys and disordered dielectrics become worse.

An analysis of the heat flow in a typical 1.75 mm² packaged GASFET sketched in Fig. 2 has been performed using the thermal resistance equations of Cooke [11] with material thermal conductivities published in various references (GaAs [12], alumina and gold [13], Kovar and iron alloys [14]). Results are summarized in Table I which also gives material conductivities used in the calculations.

At temperatures down to 20 K the total thermal resistance decreases substantially for the configuration of Fig. 2. The heat flow medium shifts in the substrate from alumina to gold metallization (assumed 5 μm thick). It is

thus important that the gold metallization and plating be thick, pure, and free of voids. A case designed for cryogenic operation should have pure silver or copper source leads and a sapphire or crystalline quartz substrate.

It is important that the chip be solder-bonded to a metallized substrate with the metallization continuing to the source leads. This is not the case in all commercially available devices. A calculation of a solder-joint thermal resistance shows it to be negligible even at 4 K. However, a silver-loaded epoxy joint of 25- μm thickness would add 300 K/W at 20 K [16].

It is also important that the total heat path from chip, thru package to amplifier case, and on to cooling station be carefully considered; this often conflicts with the desired microwave design. A chip GASFET soldered to a high-purity copper amplifier case is an excellent solution to thermal problems above 20 K but is not a necessity; a packaged device can be used.

At 4 K the thermal problem within the GaAs chip is quite severe due to boundary scattering of phonons [17, p. 149] which produces a thermal resistance increasing as T^{-3} for temperatures below 20 K. A channel with 20–50 mW of power dissipation will stabilize at a temperature of ~ 15 K even if the chip boundaries are at 4 K; hence little is gained compared to 20 K cooling. The value of the chip thermal resistance at 4 K given in Table I is only a rough approximation as the problem becomes complex. The thermal conductivity is no longer a point property of the material; the heat conduction is by acoustical waves and wave transmission and reflection at boundaries must be considered. However, an effective thermal conductivity dependent upon the object size can be defined (see Callaway [15]) and has been used in Table I with the size parameter set equal to a gate length of 0.7 μm . It should be noted that the chip thermal resistance would not be significantly reduced by immersion in normal liquid helium which has insufficient thermal conductivity for the area and heat flux involved (Though, super-fluid helium at a temperature below 2.2 K would be effective).

There is a possibility that a detailed study of the heat conduction mechanism from the channel at 20 K would show increased heating due to the small size effects discussed above which are certainly present at 4 K. Experimental evidence against this, however, is the fact that for most devices evaluated the amplifier noise temperature variation with dc bias power dissipation is small at cryogenic temperatures and similar to the variation at room temperature.

A different conclusion regarding self-heating at cryogenic temperatures was reached by Sesnic and Craig [56] who predict large self-heating for the 4 K–77 K temperature range due to poor conductivity of the Kovar source leads. Their paper did not consider the strong effects of plating on the source leads or the boundary-scattering decrease in chip thermal conductivity. These erroneous results were applied by Brunet–Brunol [57] who then attributed the lack of change of GASFET electrical characteristics below 77 K to self-heating.

III. DC CHARACTERISTICS VERSUS TEMPERATURE

The dc characteristics of a GASFET can be analyzed to determine parameters such as transconductance and input resistance which enter directly into the noise temperature equation, and also device fabrication parameters such as channel thickness a and carrier density N , which affect the noise temperature in a more complex manner. In addition, by measuring the variation of dc parameters with temperature, the variation of material parameters such as mobility μ and saturation velocity v_s , can be determined; these also enter into the noise theory.

The curves of drain current versus drain voltage at steps of gate voltage for three different manufacturers of GASFET's at 300 K and 20 K are shown in Fig. 3. In general, there is only a mild change in the characteristics of all devices tested with most changes occurring between 300 K and 80 K. The dominant effects are an increase in transconductance, saturation current, and drain conductance.

A more detailed analysis of a sample device, the Mitsubishi MGF 1412, will be performed using, with some modification, the methods of Fukui [18]. Microwave noise measurements of the identical device are described in the next section. The total channel width Z was measured with a microscope and found to be $400 \mu\text{m}$ in two $200\text{-}\mu\text{m}$ stripes and the gate length L has a published [34] value of $0.7 \mu\text{m}$ (the gate length has only a minor effect on the quantities evaluated in this section, but is important for the noise analysis). All dc data were measured at five temperatures utilizing 0.1-percent accuracy digital meters. The results are given in Table II and discussed below.

A. Forward-Biased Gate Characteristics

The forward-biased gate junction was first evaluated to find the barrier potential V_B , Schottky ideality factor n , and gate-plus-source resistance $R_g + R_s$. This was performed by measuring the gate-to-source voltage V_{gs} for forward gate currents of $0.1 \mu\text{A}$ – 10 mA in decade steps, all with drain current $I_d = 0$. The results were fitted to a normal Schottky-barrier current–voltage characteristic with V_B replaced by V_B/n as suggested by Hackam and Harrop [19]. The resulting values for V_B show little variation with temperature, in agreement with the results of others [19], [20]. The n factor increases by a large amount as temperature decreases; this is due to tunneling through the narrow, forward-biased depletion layer [21], [22] and does not effect the reverse diode characteristics and normal FET operation. When tunneling is present the n factor will vary slightly with current (i.e., the I – V characteristic is not exponential) if the doping density is not uniform. This limits the accuracy of the determination of n and hence, of V_B and $R_g + R_s$. The n values given in Table II are for the 1 – $10\text{-}\mu\text{A}$ range.

The value of $R_g + R_s$ is determined from the I_g – V_{gs} measurements in the 0.1 – 20-mA range. At these currents the voltage drop across $R_g + R_s$ becomes significant compared to the exponential ideal diode characteristic, and hence $R_g + R_s$ can be determined. However, R_g at these

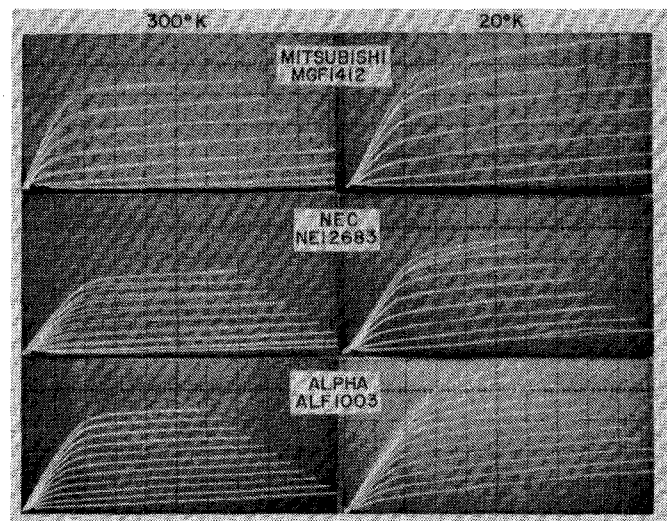


Fig. 3. Drain current, 20 mA per vertical division, versus drain voltage, 0.5 V per horizontal division, for 0.2 V steps of gate voltage for 3 manufacturers of GASFET's at 300 K and 20 K . The top curve in each photograph is at 0 V gate voltage.

TABLE II
DC PARAMETERS VERSUS TEMPERATURE FOR THE MITSUBISHI
MGF 1412 GASFET (UNITS ARE IN VOLTS, OHMS,
MILLIAMPERES, AND MILLIMHOS)

Quant	300°K	228°K	151°K	81°K	21°K
V_B	.796	.811	.834	.810	.782
n	1.125	1.216	1.47	2.0	7.2
R_g	2.66	1.7	1.5	1.4	1.2
R_s	2.3	2.3	2.1	2.1	2.2
R_d	2.1	2.4	2.5	2.4	2.4
R_t	8.8	8.8	9.3	11	$10\text{-}14$
V_p	1.226	1.151	1.156	1.172	1.159
I_o	67.8	74.3	79.1	84.7	86.2
I_s	255	279	297	318	324
g_m'	39	44	47	50	55
g_m	43	49	52	56	62
v_s/v_{so}	1.0	1.13	1.18	1.27	1.32
g_m/g_{mo}	1.0	1.14	1.21	1.30	1.44

currents is nonlinear due to the distributed gate metallization resistance. A distributed ladder network of resistors and diodes must be considered. At high currents the potential drop across the metallization resistance produces a reverse bias which results in less current through the diodes at the end of the ladder away from the gate connection point; the effective value of R_g decreases with current. This situation is described by a nonlinear differential equation which has been solved and the results have been used to find the constant, low-current value of $R_g + R_s$. The solution will be described in a separate publication [54]. The small-signal value of $R_g + R_s$ at 10-mA bias current was also measured at 100 kHz and 10 MHz . Values equal to the dc slope resistance were ob-

tained, thus assuring that thermal errors are not present in the dc measurement.

To separate R_g and R_s and also determine the drain series resistance R_d , the gate-to-source voltage V_{gsd} with drain connected to source was measured along with the gate-to-drain voltage V_{gd} with the source open; both of these values are at a gate current of 10 mA. By differentiating these quantities with V_{gs} , also measured at $I_g = 10$ mA, R_s and R_d are obtained as

$$R_s = \Delta R_1 + \sqrt{(\Delta R_1)^2 + \Delta R_1 \cdot \Delta R_2} \quad (1)$$

and

$$R_d = \Delta R_2 + R_s \quad (2)$$

where $\Delta R_1 = (V_{gs} - V_{gsd})/0.01$ and $\Delta R_2 = (V_{gd} - V_{gs})/0.01$. Note that since only voltage differences are measured the values can be highly accurate and do not depend on removing the exponential portion of the $I_g - V_g$ characteristic, as is the case with the determination of $R_g + R_s$, and therefore R_g .

The values of R_s and R_d show little variation with temperature. This is to be expected, since for a highly doped semiconductor, both the carrier density and mobility show little variation with temperature even at temperatures as low as 2 K [23], [24]. The mobility is limited by impurity scattering and carriers do not "freeze out" because the impurity band overlaps the conduction band. The gate resistance R_g decreases from 2.7 Ω at 300 K to 1.2 Ω at 21 K since it is primarily due to the resistivity of aluminum which decreases by a large amount dependent upon its purity. The theoretical resistance of the gate metallization, using the formula of Wolf [25] is 1.7 Ω at 300 K and <0.001 Ω at 21 K indicating that ~1 Ω is due to impurities or semiconductor resistance.

B. Drain Voltage-Current Characteristic

A second check on mobility variation is obtained by measurements in the linear region (i.e., no velocity saturation) of the $I_d - V_d$ characteristic. The drain current I_d was measured for $V_{gs} = 0$ and $V_d = 50$ or 100 mV. $R_t = V_d/I_d$ is reported in Table II and shows somewhat more variation with temperature than R_s or R_d (which are contained in R_t). In particular the value at 21 K is dependent upon past history; it is lower by ~30 percent after forward biasing the gate junction. This has not been explained. No such "memory" effect is observed in the device at normal bias levels.

The saturated drain current I_0 at $V_{gs} = 0$ and $V_d = 3$ V was measured along with the gate voltage $-V_p$ to bring the drain current down to 2 mA; V_p is a good approximation to the pinch-off voltage of the device. These quantities, measured at 300 K, can be used to determine the doping density N , and channel thickness a of the device through the well-established relations

$$V_p + V_B = \frac{qNa^2}{2\kappa\epsilon_0} \quad (3)$$

$$I_s = qv_s NaZ \quad (4)$$

where $q = 1.6 \times 10^{-19}$ C, $\epsilon_0 = 8.85 \times 10^{-14}$ F/cm, $\kappa = 12.5$ for GaAs, $Z = 0.4$ mm, and the saturated velocity v_s is assumed to be 1.4×10^7 cm/s. The quantity I_s is the open-channel saturation current and is related to I_0 [18] by

$$I_s = I_0/\gamma \quad (5)$$

where

$$\gamma = 1 + \sigma - \sqrt{\delta + 2\sigma + \sigma^2} \quad (6)$$

$$\delta = (V_B + 0.234L)/(V_B + V_p) \quad (7)$$

$$\sigma = 0.0155R_s Z/a \quad (8)$$

and a and L are in micrometers and Z is in millimeters. The channel thickness a is not initially known for use in σ but since it is a moderately small correction factor, an initial estimate can be used and later iterated. Solving (3) and (4) for a and N gives $a = 0.10$ μm and $N = 2.9 \times 10^{17}/\text{cm}^3$, in good agreement with information supplied by the manufacturer [26].

The measured insensitivity to temperature of $V_p + V_B$ verifies through (3) that N is not a function of temperature. The temperature dependence of I_s must then be due to a change in saturation velocity v_s ; its value relative to the 300 K value is given in Table II. The results are in general agreement with the increase in saturation velocity measured by Ruch and Kino [27] in the 340 K–140 K range.

Finally, the transconductance g'_m was measured by taking 50-mV increments in V_g above and below the low-noise bias point of $V_d = 5$ V, $I_d = 10$ mA. This must be corrected for effects of source resistance to give the true transconductance $g_m = g'_m/(1 - g'_m R_s)$; both g'_m and g_m are given in Table II in units of millimhos. The values are approximately 35 percent lower than those given by the approximate theoretical expression

$$g_m = \frac{I_s}{2(V_p + V_B)} \cdot \frac{1}{(1 - I_d/I_s)} \quad (9)$$

and the exact theoretical curve given in [28, fig. 12(c)] (which is a little closer). Fukui had a similar problem in the analysis of his data [18, p. 787]. The increase in measured transconductance with decreasing temperature follows the saturation velocity increase determined from measurements of I_0 , V_p , and V_B .

IV. MICROWAVE PERFORMANCE VERSUS TEMPERATURE

A. Gain and Noise Measurement Procedure

A block diagram of the test configuration used for measurements of gain and noise temperature of cooled amplifiers is shown in Fig. 4. Auxiliary equipment such as a network analyzer, reflectometer, and spectrum analyzer were used for impedance, return loss, and spurious oscillation measurements. At a later stage of the work an HP 9845 calculator and HP 346 avalanche noise source were incorporated to allow a swept frequency plot of 50 noise temperature and gain measurements to be performed in

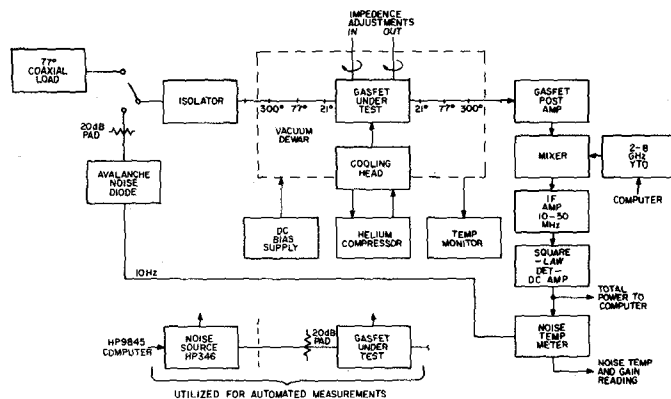


Fig. 4. Test setup for noise and gain measurements of cooled amplifiers. The automated measurement procedure gives a swept-frequency output of noise temperature (corrected for second-stage contribution) and gain; this replaced the hot load-cold load manual method after corroboration of results was established.

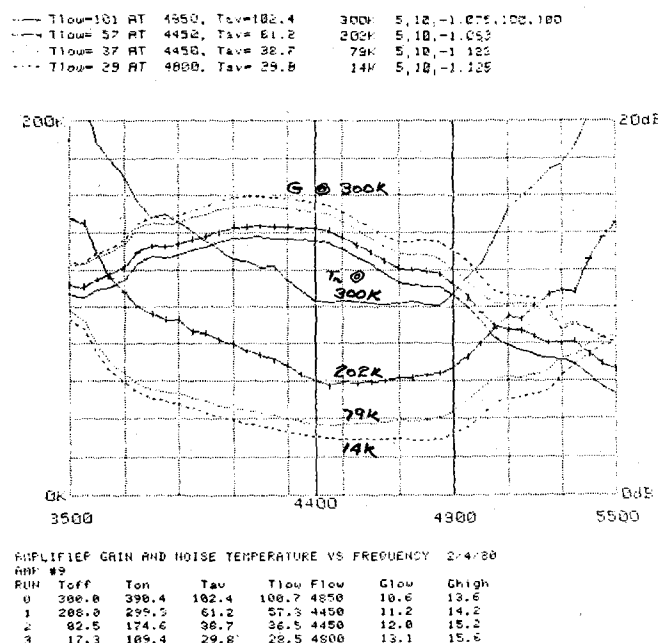


Fig. 5. Noise temperature and gain versus frequency for the Mitsubishi MGF 1412 transistor at several physical temperatures. This is a direct copy of the on-line output of an automated measuring system utilizing an Hewlett-Packard 9845 computer. The results are first plotted on a CRT and then can be copied on a thermal printer. Tabulated below the plot are noise-source-off temperature, noise-source-on temperature, average amplifier noise temperature between markers at 4.4 and 4.9 GHz, lowest noise and its frequency, and lowest and highest gain between marker frequencies. The lowest and average noise temperatures are also given above the plot area along with a space for user comments which in this case are physical temperature, drain voltage and current, and gate voltage.

20 s; a typical output from this automated system is shown in Fig. 5. The amplifiers under test were cooled by a commercially available [29] closed-cycle refrigerator with a capacity of 3 W at 20 K and a cool-down time of 5 h.

A large error in the noise temperature measurement of a mismatched amplifier can result if the source impedance changes when switching from hot load to cold load. For this reason an isolator is used between the loads and

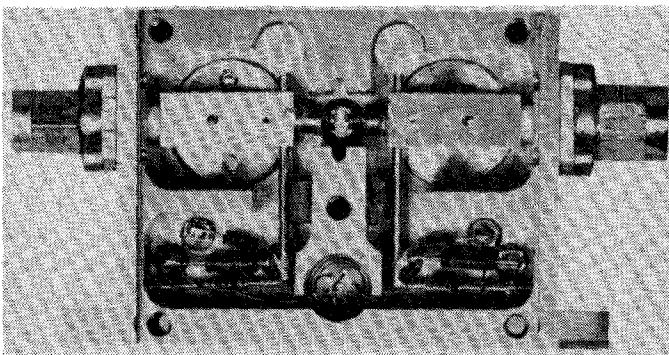


Fig. 6. Test amplifier with adjustable source and load resistance. The spacing between the $\lambda/4 = 15.9$ -mm long rectangular slab transmission line and ground plane is adjusted by turning the circular threaded slug. DC blocking capacitors are realized by teflon coating the SMA connector center pin where it enters the slab. The slab transmission line is supported by the coaxial connector, a chip capacitor, and a teflon bushing held by a nylon screw. The transistor is mounted by its source leads on a 6.3-mm diameter threaded copper slug with center 5.7 mm from the end of each $\lambda/4$ line.

amplifier input. The total loss from 77 K liquid-nitrogen cooled load to the amplifier was accurately measured and corrected for. This included 0.62 dB in the coaxial switch, isolator, and SMA hermetic vacuum feed thru; 0.11 dB in a stainless-steel outer-conductor beryllium-copper inner-conductor coaxial line transition from 300 K to 20 K; and 0.07 dB in 10 cm of internal coaxial line at 20 K.

For the automated measurements an HP 346 calibrated avalanche diode was used in cascade with a modified HP 8493A coaxial attenuator. No isolator is necessary. The attenuator is modified for cryogenic use [30] by replacing the conductive-rubber internal contacts by bellows contacts [31], drilling a vacuum vent hole in the body, and tapping the body for mounting a temperature sensor [32]. The change in attenuation of the modified 20-dB attenuator upon cooling from 300 K to 77 K is a decrease of 0.05 ± 0.03 dB; it is assumed that negligible change will occur upon further cooling to 20 K as this is typical for most resistance alloys. The attenuator may be purchased calibrated from Hewlett Packard (Option 890); however, the contact modification necessitates a recalibration (attenuation at 300 K decreased by 0.05 dB) and was performed with a digital power meter. For an amplifier with 30 K noise temperature the cooling of the attenuator from 300 K to 20 K provides a factor of $(300+30)/(20+30) \sim 6$ decrease in error of the amplifier noise temperature measurement due to noise source or attenuator errors. For this case a noise temperature error of $\pm 2.3^\circ$ results from an uncertainty of noise source excess noise plus attenuator error of ± 0.2 dB. The agreement between amplifier noise measurements made with the hot/cold loads and the HP 346 noise source was within ± 2 K for cooled amplifiers and ± 5 K for uncooled amplifiers.

In order to determine the optimum source resistance and load resistance as a function of temperature, a test amplifier having variable impedance quarter-wave transformers at input and output was constructed and is shown in Fig. 6. A schematic of this amplifier and of all other

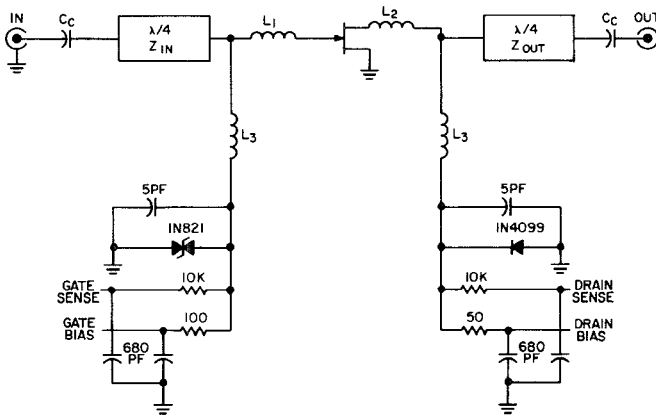


Fig. 7. Schematic of all amplifiers discussed in this paper. The bias decoupling inductance L_3 is realized by $\lambda/4$, $Z_0 = 100 \Omega$ line in the test amplifier; in other amplifiers it is a small coil described in the text.

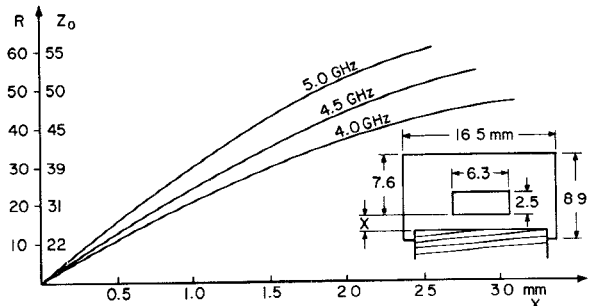


Fig. 8. Characteristic impedance Z_0 and source resistance, $R = Z_0^2/50$, as a function of spacing X from threaded-slug ground plane to $\lambda/4$ slab transmission line having cross section shown in figure.

amplifiers described in this paper is shown in Fig. 7. The variable impedance line consists of a slab transmission line having cross section as shown in Fig. 8 and a movable ground plane realized as a threaded slug with a diameter of $\lambda/4$. The slug is slotted and has a thread-tightening screw to assure ground contact and to lock the position. Calibration of the characteristic impedance versus slug position was performed by utilization of a miniature coaxial probe inserted in place of the FET and connected to a network analyzer; results are given in Fig. 8. The loss of the $\lambda/4$ line was calculated to be less than 0.025 dB at $Z_0 = 22 \Omega$ using the microstrip loss formulas of Schneider [33].

B. Results

As a first step, the noise temperature of several commercially available GASFET's was measured at a frequency of ~ 4.5 GHz from 300 K to 20 K; results are shown in Fig. 9. At each temperature bias and source resistance were optimized for minimum noise; the changes were not large. For all units the peak gain was ~ 12 dB at 300 K and increased by 1 or 2 dB at 20 K. The measurement frequency was chosen for minimum noise at 300 K and no change in the optimum frequency was noted as temperature decreased.

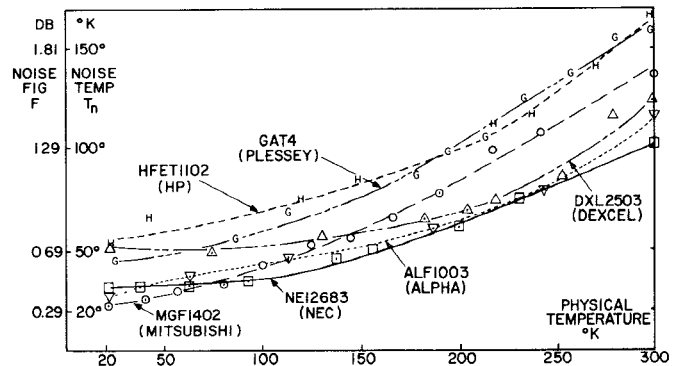


Fig. 9. Noise temperature versus physical temperature for several manufacturers of GASFET's. Only one or two samples of the HP, Dexcel, Alpha, and Plessey devices were evaluated, and units from another batch may give better cryogenic performance.

On the basis of these tests and because of its high burnout level [34], the Mitsubishi device was selected for detailed study and for use in the construction of amplifiers needed for use in radio astronomy. A selected version of the MGF 1402, the MGF 1412, became available and was used for further tests; it has lower noise temperature (~ 100 K) at 5 GHz and 300 K, but has a noise temperature at 20 K close to that of the MGF 1402. Of approximately 15 samples of the MGF 1412 tested at 20 K, the noise temperature was between 15 K and 27 K.

The gain and noise temperature of a MGF 1412 at four temperatures between 300 K and 14 K is shown in Fig. 5; dc parameters for the same device are given in Table II. As the amplifier is cooled, the gain increases by 2.0 dB. This is less than the 3.0-dB increase of g_m because of internal negative feedback (which stabilizes the gain against g_m changes) and possibly because of a reduction in parallel output resistance. As the noise temperature decreases, the bandwidth for a given increase in noise temperature increases, but there is very little other change in frequency response of either gain or noise temperature.

A complete comparison of noise theory and experiment requires the measurement of four noise parameters of the device. There are many sets of four parameters which can be compared. The set which is most directly measured is the minimum noise temperature T_{\min} , the optimum source impedance $R_{\text{opt}} + jX_{\text{opt}}$, and the noise conductance g_n . These relate to the measured data in Fig. 10 of noise temperature T_n as a function of source impedance $R + jX$ by

$$T_n = T_{\min} + T_0 \cdot g_n \cdot \frac{[(R - R_{\text{opt}})^2 + (X - X_{\text{opt}})^2]}{R} \quad (10)$$

where $T_0 = 290$ K.¹

The values of R , R_{opt} , X , X_{opt} , and g_n are dependent upon the choice of reference plane between device and

¹In this paper $T_0 = 290$ K independent of ambient temperature which will be denoted as t : T_0 . Several papers in this field normalize quantities which are not functions of temperature to ambient temperature (using the symbol T_0), producing a normalized quantity which is a function of temperature and confusing the reader.

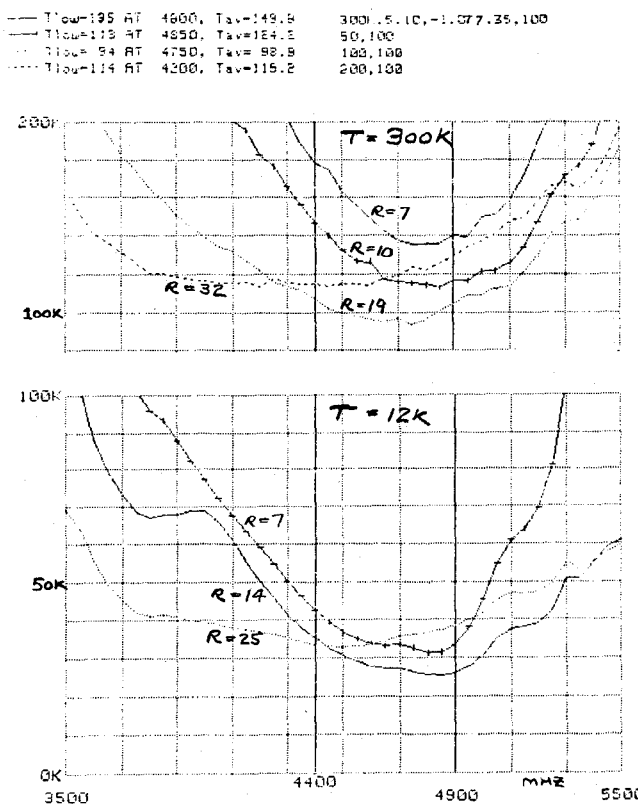


Fig. 10. Noise temperature versus frequency for various source resistances and Mitsubishi MGF 1412 GASFET at 300 K (top) and 12 K (bottom, note change in temperature scale.) Device bias was $V_{ds}=5$, $I_d=10$ mA at both temperatures.

source but T_n and T_{min} are not for a lossless coupling circuit. Values for two reference planes defined in Fig. 11 are presented in Table III. The first and fifth columns are for a reference plane at the gate-lead case interface of the packaged device; the second and sixth columns are for the GASFET chip and thus the effects of case capacitance and gate bonding wire inductance have been removed. These "chip" columns should be compared with the theoretical columns which will be discussed in Section V.

C. Impedance Measurements

The noise theory to be discussed in the next section expresses the four noise parameters in terms of material parameters, dc bias values, device dimensions, and the equivalent circuit elements R_m , R_i , R_s , g_m , and C_{gs} , shown in Fig. 11. The values of $R_m + R_i = R_g$, R_s , and g_m , all measured at dc, are given in Table II. The capacitance, $C_{gs} + C_{gd}$, was measured at 1 MHz as a function of V_{gs} with a precision capacitance bridge [35]; a value of 0.75 pF was obtained at the low-noise bias of $V_{gs} = -1.1$ V. This includes case capacitance, which was then removed by measuring a defective device with the gate bonding wire lifted off the chip; a value of 0.25 pF was obtained for the case capacitance.

The above dc resistances and 1-MHz capacitances, together with a skin effect correction to R_m and an estimate of R_i , will be used in the comparison of theoretical and measured noise parameters. Attempts were made

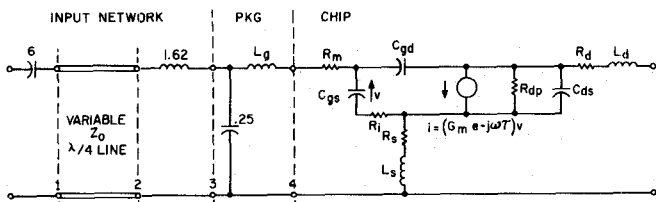


Fig. 11. Equivalent circuit of amplifier input circuit and Mitsubishi MGF 1412 transistor. The element values are based upon dc resistance measurements, 1-MHz capacitance measurements, and three sets of S parameters measured in different test fixtures. The resistance R_i cannot be separated from R_m by these measurements since the reactance of C_{gd} is so high; the value of R_i is an estimate. The error values are conservative estimates based upon analysis of all the data.

TABLE III
MEASURED AND THEORETICAL 4.9-GHZ NOISE PARAMETERS OF
MITSUBISHI MGF 1412 AT 300 K AND 20 K

Symbol	Expt Pkg 300°K	Expt Chip 300°K	Pucel Theory 300°K	Fukui Formula 300°K	Expt Pkg 20°K	Expt Chip 20°K	Pucel Theory 20°K
T_{min}	91 ± 3	91 ± 3	72	151	25 ± 2	25 ± 2	16
R_{opt}	20 ± 2	63 ± 6	74	22	15 ± 1	47 ± 3	41
X_{opt} $= -X_c$	55 ± 5	101 ± 9	119	42	58 ± 5	107 ± 10	104
$1/g_n$	100 ± 20	205 ± 40	668	727	370 ± 30	800 ± 100	1800
R_n	34 ± 8	69 ± 18	29	3.1	10 ± 2	17 ± 3	6.9
r_n	$3.8 \pm .6$	15 ± 3	8.2	-38	$0.6 \pm .2$	2.6 ± 1	0.9
R_c	-4 ± 5	-31 ± 15	8.1	167	0.9 ± 4	-13 ± 10	7.9

to determine $R_m + R_i$ and C_{gs} by microwave S -parameter measurements, to be described next, but the results were variable and more confidence is placed in the low-frequency measurements. The skin-depth of aluminum at 5 GHz is $1.2 \mu\text{m}$ which should be compared with the gate metallization thickness of $0.7 \mu\text{m}$. The dc value of R_g is 2.7Ω and its value at 5 GHz is estimated to be 5Ω ; this estimate is partially influenced by the S -parameter results which gave 4.3 to 12.7Ω . The gate-charging resistance R_i is estimated to be 1Ω by noting that R_s and R_d have values of 2.3 and 2.1Ω and R_i occurs over a length somewhat shorter than R_s and R_d . It should be noted that R_i is of second order importance to the noise results but the fact that R_m is determined by subtracting R_i from the measured R_g is of somewhat greater importance. The final value of R_m is $4 \pm 2 \Omega$ and this error value limits the accuracy of comparison of noise theory and experiment.

The S parameters of a packaged device were measured from 2 to 18 GHz on computer-corrected automatic network analyzers at two organizations [36], [37] with different test fixtures and calibration procedures; a third set of S parameters is reported on the MGF 1402 data sheet. The input capacitance at 2 GHz determined from each of the three S -parameter sets was within 0.06 pF of the 1-MHz capacitance measurement. However, above 8 GHz the measured S parameters diverge, probably due to reference plane definition problems. The COMPACT program [59] was used to optimize circuit elements to give mini-

mum weighted mean-square error between circuit and measured S parameters in the 2–10-GHz range. Some of the elements determined in this way have large variability dependent upon the data set used and details of the fitting procedure. As a relevant example, the value of R_g changed from 12.7Ω to 7.8Ω dependent upon whether R_s was fixed at 2.3Ω or allowed to vary in the optimization procedure (which gave $R_s = 1.0 \Omega$). Using S parameters measured with a different analyzer gave $R_g = 6.7$ and 5.4 for R_s fixed and variable, respectively.

The reasons for the variability of the R_g value are its small resistance relative to the reactance of C_{gs} and also the strong dependence of the input resistance upon the small feedback elements C_{gd} , L_s , and R_s . Our conclusion is that it is very difficult to determine R_g from S -parameter measurements at normal bias values; a careful measurement of S_{11} with $V_{ds} = 0$ (and hence $g_m = 0$ and no feedback effects) may be more successful.

V. NOISE THEORY

A. Summary of Present GASFET Noise Theory

A comprehensive paper covering the history, dc, and small-signal properties, and an exhaustive but not conclusive treatment of noise in microwave GASFET's was written in 1975 by Pucel *et al.* [28]. The noise treatment includes the induced gate noise mechanism of Van der Ziel [38], the hot-electron effects introduced by Bachtold [39], and presents as new, the mechanism of high-field diffusion noise due to dipole layers drifting through the saturated-velocity portion of the channel. This latter mechanism along with the thermal noise of parasitic resistances R_m and R_s in the input circuit was found to be the dominant source of noise in modern, short-gate-length GASFET's at room temperature.

The above paper predicts the correct dependence of noise upon drain current and, by adjustment of a material parameter D , which describes the diffusion noise but is not accurately known from other theory or experiments, a good fit to measured 4-GHz data is presented. However, the theory does not agree with experimental data at the low end of the microwave spectrum (<3 GHz) where a linear dependence of noise temperature upon frequency is predicted but not observed. It was suggested that this noise may be due to traps at the channel–substrate interface but devices with a buffer layer such as the NEC 244 also show the excess low-frequency noise [40]. The temperature dependence of the low microwave frequency noise also does not agree with the trap assumption [41]. A recent work by Graffeuil [42] attributes the low-frequency noise to frequency dependence of hot-electron noise and also matches experimental data without invoking the high field diffusion noise which is dominant to the Pucel *et al.* theory.

The four noise parameters T_{\min} , R_{opt} , X_{opt} , and g_n define the noise properties of any linear two-port and all other noise parameters can be derived from them. Other

noise parameters which appear in GASFET noise theory are the noise resistances R_n and r_n , and correlation impedance $R_c + jX_c$. Here, R_n is proportional to the total mean square noise voltage in series with the device input, and r_n is proportional to the portion of this noise voltage which is uncorrelated with the current noise represented by g_n . (It should be remarked that the symbol R_n is used to represent a noise voltage source that is not in series with the input but is called the “input noise resistance” in some papers [38], [41].) The following relations between these quantities can be easily derived using the definitions given by Rothe and Dahlke [43]:

$$R_n = g_n |Z_{\text{opt}}|^2 \quad (11)$$

$$R_c = \frac{T_{\min}}{T_0} \frac{1}{2g_n} - R_{\text{opt}} \quad (12)$$

$$X_c = -X_{\text{opt}} \quad (13)$$

$$r_n = g_n (R_{\text{opt}}^2 - R_c^2) \quad (14)$$

$$r_n = \frac{T_{\min}}{T_0} \left(R_{\text{opt}} - \frac{T_{\min}}{T_0} \frac{1}{4g_n} \right). \quad (15)$$

The experimental results of the previous section will be compared with the Pucel *et al.* theory and also with the empirical equations of Fukui which are based upon fitting noise data to Bell Telephone Laboratory GASFET's at 1.8 GHz [44]. The theoretical results for the four noise parameters T_{\min} , R_{opt} , X_{opt} , and g_n , which are most directly measurable are expressed in terms of intermediate parameters r_n and R_c as follows [28]:

$$g_n = K_g / g_m X_{gs}^2 \quad (16)$$

$$r_n = t(R_m + R_s) + K_r / g_m \quad (17)$$

$$R_c = R_m + R_s + K_c R_t \quad (18)$$

$$R_{\text{opt}} = (R_c^2 + r_n / g_n)^{1/2} \quad (19)$$

$$X_{\text{opt}} = K_c |X_{gs}| \quad (20)$$

$$T_{\min} = 2T_0 g_n (R_c + R_{\text{opt}}) \quad (21)$$

where t is the ratio of device physical temperature to 290 K, $X_{gs} < 0$ is the reactance of the gate-to-source capacitance, and the three K 's are noise coefficients which are given in [28] as functions of bias, device dimensions, and material parameters. K_g is proportional to the squared magnitude of the equivalent current source in the input circuit and represents the induced gate circuit noise current as well as the correlated² current needed to represent noise in the drain circuit. The uncorrelated noise resistance r_n contains a first term due to thermal noise in $R_m + R_s$ (and hence proportional to t as suggested in [28]) and a second term which, through K_r , is a measure of the noise voltage necessary to represent uncorrelated drain current noise.

²The words correlated and uncorrelated can refer to correlation between voltage and current sources in a Rothe–Dahlke noise representation or to correlation between gate current noise and drain current noise; an asterisk (*) will be used when the latter is meant.

TABLE IV
EXPERIMENTAL AND THEORETICAL NOISE COEFFICIENTS OF
MGF 1412 AT 300 K AND 20 K

Qty	Expt 300°K	Theory 300°K	Expt 20°K	Theory 20°K
K_g	0.89	0.27	0.33	0.15
K_c	1.55	1.83	1.65	1.60
K_r	0.36	.072	0.13	.03
P	2.50	.98	1.02	0.403
R	0.64	.26	0.27	0.082
C	0.893	0.961	0.917	0.935

It is important to note that the K noise coefficients are independent of frequency except for the possible frequency dependence of material parameters (high field diffusion coefficient D , saturated velocity v_s , hot-electron noise coefficient δ , and mobility μ). The noise coefficients are convenient for describing the measured noise performance of a device but three other coefficients P , R , and C are more directly related to the noise generation mechanisms. The mean-square drain current noise is proportional to P and the mean-square gate current noise is proportional to R ; the correlation* coefficient between these two is C . The relations between the coefficients are given in [28] and are repeated below in an algebraically simplified form

$$K_g = R + P - 2C\sqrt{RP} \quad (23)$$

$$K_g K_c = P - C\sqrt{RP} \quad (24)$$

$$K_g K_r = RP(1 - C^2). \quad (25)$$

B. Comparison of Experimental Results with Theory

The experimental results and theory are compared in Tables III and IV. The theoretical values are obtained using the measured values of g_m and I_s from Table II and R_i , R_m , R_s , and C_{gs} from Fig. 11 (rather than values which could have been computed from device dimensions, and material parameters). The device channel thickness, $a=0.10 \mu\text{m}$, and doping density $N=2.9 \times 10^{17}$, were determined from the dc measurements. The gate length, $L=0.7 \mu\text{m}$, was measured; this value is also reported in [34]. The material parameter values are those used in [28] ($D=35 \text{ cm}^2/\text{s}$, $\delta=1.2$, $E_s=2.9 \text{ kV/cm}$, $v_s=1.3 \times 10^7 \text{ cm/s}$, and $\mu_0=4500 \text{ cm}^2/\text{V}\cdot\text{s}$). The device was operated with $V_{ds}=5 \text{ V}$, $I_d=10 \text{ mA}$, and $V_{gs}=-1.081$ at 300 K and -1.123 at 20 K; these values gave minimum noise at both temperatures. It is, of course, the experimental values corrected to the chip reference plane which should be compared with theoretical results, which do not include package parasitics.

The last column of Table III gives the theoretical results of Pucel *et al.* modified in the following way for application at 20 K.

1) The thermal noise in the parasitic resistances $R_m + R_s$, has been reduced by the factor $t=20/290$ in (17). This reduces T_{\min} from 72 K to 40 K.

2) The transconductance g_m has been replaced by the 20 K measured value (an increase from 0.043 to 0.062 mhos)

and the saturation velocity v_s , and saturation field E_s , have been increased by a factor of 1.32 as deduced from the measured dc parameter changes. This further reduces T_{\min} from 40 K to 26.5 K.

3) Thermal noise within the channel has been reduced by multiplying the Pucel factors P_0 , R_0 , and S_0 used to calculate the K noise coefficients by t ; this brings T_{\min} to 15.7 K.

4) As points of additional theoretical interest, if t is made equal to zero both for the external and internal thermal noise, T_{\min} reduces from 15.7 K to 11.2 K; i.e., the theoretical coefficient of noise temperature versus physical temperature is 0.22 K per K at cryogenic temperatures. Also, if $D=0$ (no high-field diffusion noise) $T_{\min}=5.0$ K. Thus at 20 K and at the experimental bias value which gives lowest noise temperature, approximately 1/3 of the total noise is contributed by each of the mechanisms of thermal, high-field diffusion, and hot-electron noise. This is conceptually only a rough approximation since the noise contributions to T_{\min} are not additive; at each step above (i.e., $t=0$ or $D=0$) the source impedance has a new optimum which changes the contributions from remaining noise mechanisms. Perhaps a more meaningful comparison would be for T_n at a fixed source impedance.

Several authors [41], [42], [53] find the hot-electron noise coefficient δ to be a strong function of temperature but this is primarily because the nonthermal portion of the hot electron noise has been normalized to ambient temperature (see footnote 1). Our results suggest that a convenient form for the electron temperature T_e is

$$T_e = T_0 [t + f(E)] \quad (26)$$

where $T_0=290$ K (and cancels out in the noise figure expression) and $f(E)$ is the nonthermal noise dependent upon electric field but only weakly dependent upon temperature. For the last column of Table III, $f(E)=\delta(E/E_s)^3$ has been used with $\delta=1.2$ and $E_s=3800 \text{ V/cm}$ (compared to $E_s=2900 \text{ V/cm}$ at 300 K). A better fit to experimental data would be achieved if either δ were higher or E_s lower at 20 K. Experimental evidence for the increase of $f(E)$ by a factor of ~ 2.5 at cryogenic temperatures is contained in our own unpublished measurements on millimeter-wave GaAs mixer diodes and also in the measurements of Keen [55].

Further insight into the noise temperature limitation at cryogenic temperatures can be gained by examining an approximate form of the minimum noise temperature equation

$$T_{\min} = 2T_0 \cdot \sqrt{K_g} \cdot \omega C_{gs} \cdot \sqrt{\frac{t(R_m + R_s)}{g_m} + \frac{K_r}{g_m^2}} \quad (27)$$

which is valid for $K_g R_c^2 / X_{gs}^2 \ll t(R_m + R_s)g_m + K_r$; this approximation produces ~ 10 -percent error for the MGF 1412 data. At room temperature the first term under the large radical is dominant and K_r is not important; the noise voltage generator in the input circuit is dominated by the thermal noise of $R_m + R_s$. At cryogenic tempera-

tures where $t \rightarrow 0$ the second term K_r/g_m^2 becomes dominant (even though g_m has increased) and the noise temperature is limited by the amount of nonthermal noise coupled into the gate circuit and uncorrelated* with the drain current noise. The coefficient K_r is proportional to $1 - C^2$ where C , the correlation* coefficient, is near 1 and thus small changes in C are likely to have large effects on the cryogenic noise temperature; this will not be true at room temperature. The larger variability of the cryogenic noise temperature from one device to another may be due to this effect.

The agreement between experimental results and the theory of Pucel *et al.* for values of T_{\min} , R_{opt} , and X_{opt} is good at both 300 K and 20 K—especially if the error range for R_m is considered. Other samples of the MGF 1412 gave a lower noise temperature at 20 K (as low as 15 K) than the particular device which was evaluated in detail; this would improve the agreement with theory. The agreement with the theory is marred by a factor ~ 3 disagreement in the value of g_n . It is not known at present whether this is an experimental artifact or a failure of the theory. The value of g_n was determined from the noise temperature versus source resistance characteristic but it was also checked, with good agreement, by measuring the noise-temperature bandwidth of the data of Fig. 10. The discrepancy in g_n leads to an even larger discrepancy in the correlation resistance R_c , which depends, through (12), on the difference between $1/g_n$ and R_{opt} . The negative value of R_c which results from the measurements is physically possible (it only means the input voltage and current noise sources have a negative real part in their correlation coefficient) but is certainly in disagreement with the theory.

The experimental values of the K coefficients in Table IV were obtained by solving (16)–(21) in terms of the measured noise parameters. The coefficients P , R , and C were then obtained by solving (23)–(25) by an iteration method. The discrepancy between experimental and theoretical R_c and g_n further propagate into discrepancies in the noise coefficients. In addition, the experimental value of K_r at 300 K is subject to large error because the measured data is insensitive to K_r due to the dominance of thermal noise.

The agreement between the experimental results and the empirical equations of Fukui [44] is poor. This may be due to the fact that Fukui's equations are derived from measurements at 1.8 GHz where low-frequency noise generation mechanism has a large effect; thus the formula predicts a higher than observed noise temperature at 4.9 GHz. It may also be true that some other variables in the transistor fabrication (such as the doping profile near the substrate interface or gate metallization thickness) effect the equations. It should be noted that the Fukui noise parameter equations require the values of g_m and C_{gs} at zero gate bias; thus the measured zero bias values of 0.098 mhos and 0.75 pF have been used in Table III.

VI. EXAMPLES OF CRYOGENIC GASFET AMPLIFIERS

Several models of GASFET amplifiers for the 5-GHz frequency range and for use at 20 K have been designed. All use 1.75 mm² packaged GASFET's (usually the Mitsubishi MGF 1412), gold-plated copper (for thermal conductivity and solderability) metal parts (except for some brass contact tabs), and microstrip transmission lines with teflon-coated fiber-glass dielectric [45]. In order to avoid large thermal stresses and mechanical failures, tight and rigid connections are avoided. Metallized ceramic substrates are also avoided because of possible cracking of the ceramic or metal-film solder-joints after repeated temperature cycling.

All amplifiers utilize an external dc power regulator which automatically adjusts the gate voltage to maintain a set drain current. This requires one TL075BCM quad-operational amplifier chip per GASFET stage and provides buffered monitoring of V_{ds} , I_d , and V_{gs} . As shown in Fig. 7 bias protection circuitry is included in the microwave chassis. The 1N821 voltage-reference zener diode utilized for gate protection contains a diode which prevents forward conduction of the zener diode and thus allows the GASFET gate to be forward biased for testing; the zener diode limits negative gate bias to approximately -6 V. Both the 1N821 and 1N4099 diodes have sharper zener characteristics at 20 K than at 300 K.

A. Single-Stage Basic Amplifier

A single-stage amplifier, for use as a second stage following a cooled-paramp first stage, was required for the front ends of the very large array radio telescope [46]. The unit need not be optimized for minimum noise as the first stage gain is 15 dB. However, it must have a gain which is flat within ± 0.5 dB over the 4.5–5-GHz range, an output return loss > 10 dB, and must be highly reliable since 54 units are required in the 27-element, dual-polarization array. An input match is not required since the input will be connected through a short cable to the 5-port circulator of the paramp.

A photograph of the amplifier and some of the key parts is shown in Fig. 12. Utilizing a thermostatically-controlled hot plate, joints are soldered as follows: 1) GASFET source leads to mounting stud with pure indium solder [47] (for good thermal conductivity) and a flux [48]; 2) chip capacitors to chassis with silver-alloy flux-core solder [49]; and 3) zener-diodes and connector ground with low-temperature solder [50]. Other components are then soldered to the chip-capacitors with silver-alloy solder and a small soldering iron.

The input and output $\lambda/4$ transformers are 4.1 mm wide \times 11.2 mm long \times 0.75 mm thick microwave circuit board [45] and are held in place through slotted holes with 2-56 nylon screws. The slotted holes allow the transformer position relative to the GASFET to be adjusted to tune the center frequency of operation. Brass tabs under each

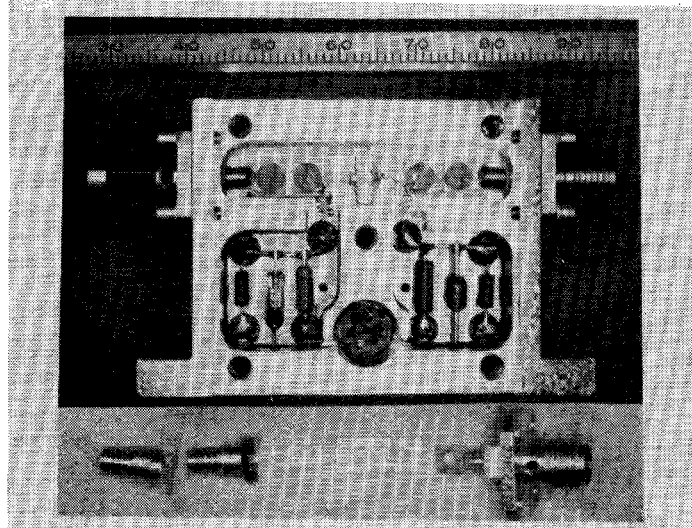


Fig. 12. Single-stage basic amplifier; scale on photograph is in units of mm. See Fig. 7 for schematic, Fig. 14 for close-up of transistor mounting stud, and text for construction details.

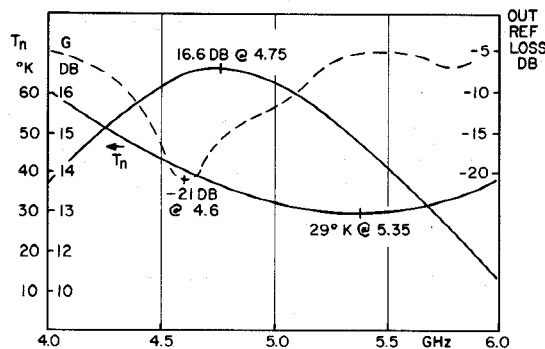


Fig. 13. Noise temperature, gain, and output return loss for single-stage basic amplifier at a temperature of 20 K.

nylon screw make connections to the SMA input and output connectors and also to the GASFET gate and source leads. Two layers of 0.02-mm thick polyester tape [51] are placed between each connector tab and the transmission line to form a dc blocking capacitor. Bias voltage for both gate and drain is fed through coils formed of 3 turns of 0.2-mm diameter phosphor-bronze wire wound with 1.25-mm inner diameter; these have high impedance relative to the circuit and are not critical.

The completed amplifier is tuned by sliding the transformers and slightly bending gate and drain leads. The drain is tuned for maximum output return loss (> 20 dB) at band center and the gate is tuned for flat-gain. This will result in a minimum noise frequency f_{\min} , 600 MHz above the gain center frequency f_0 , as shown in Fig. 13. This offset is predicted by the noise theory. For a source impedance consisting of an inductor in series with the source resistance, $f_{\min}/f_0 = \sqrt{K_c}$, assuming the drain circuit is broad band compared to the gate circuit. (Neither of these assumptions is quite true for this amplifier.) This offset may be removed with source-inductance feedback as is described next.

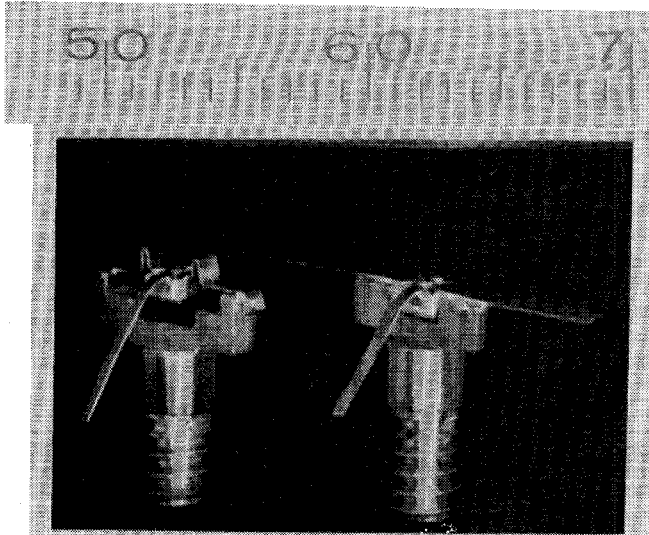


Fig. 14. Transistor mounting studs for feedback (left) and basic (right) amplifiers. Scale is in millimeters.

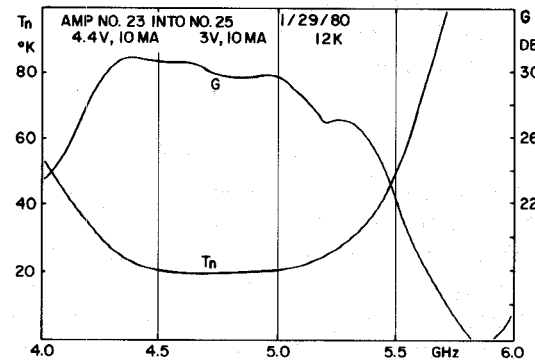


Fig. 15. Gain and noise temperature of cascade of isolator, feedback amplifier, isolator, and basic amplifier, all at 12 K. Noise temperature is 20 K over a 500-MHz bandwidth and < 25 K over a 800-MHz frequency range. Output return loss is > 10 dB from 4.5 to 5.1 GHz.

B. Single-Stage Feedback Amplifier

A small modification of the previously described amplifier results in a unit with little frequency offset between peak gain and minimum noise temperature. The modification, described in Fig. 14, is to increase the source lead inductance by widening the GASFET mounting stud and also bending small loops in the source leads. This change has little direct effect upon noise temperature but the input circuit can now be tuned to a lower resonant frequency (4.25 GHz with $V_d = 0$, 4.70 GHz with $V_d = 4.4$) giving both optimum noise and maximum gain at ~ 4.75 GHz. The gain and noise temperature of this amplifier, cascaded with the amplifier of the previous section, is shown in Fig. 15; cooled isolators are included at the input and between the two amplifiers. Output return loss is > 10 dB from 4.5 to 5 GHz without an output isolator.

The use of source lead inductance to improve input match for a ~ 1.5 -GHz amplifier has been previously described [5], [52]. At 5 GHz the situation is more complex because of effects of gate to drain capacitance and

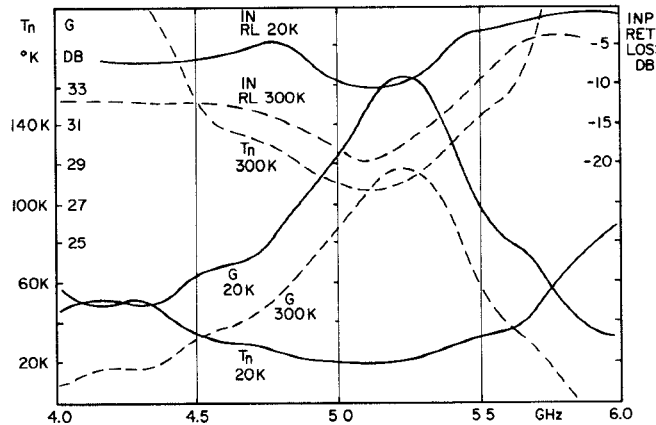


Fig. 16. Noise temperature, gain, and input return loss for two-stage feedback narrow-band amplifier described in Section IV-C at 20 K and 300 K. Output return loss at 5.0 GHz was 17 dB at 20 K and 25 dB at 300 K.

increased sensitivity of noise temperature to the reactance of the driving source. The FET source lead inductance L_s produces an effective impedance z_{FB} added in series with the input to the gate

$$z_{FB} = \frac{g_m L_s}{C_{gs}} \cdot \frac{1}{1+y_d/y_1} \quad (28)$$

where y_d is the transistor output admittance for $g_m=0$ and y_1 is the load admittance presented to the transistor. For the amplifier under consideration y_1 is adjusted so z_{FB} is primarily capacitive, the input resonant frequency is increased, and the noise-gain frequency offset is reduced to zero. At this value of y_1 the output is also matched (but $y_1 \neq y_d^*$ since y_d is for $g_m=0$) but the input is not matched. In the next section a two-stage amplifier, matched by feedback, will be described.

C. Two-Stage Feedback Narrow-Band Amplifier

An amplifier was constructed by combining in one case the single-stage feedback amplifier and the single-stage basic amplifier previously described. (With the exception that input and output $\lambda/4$ transformer width was 6 mm; interstage $\lambda/2$ line was 4.1 mm wide.) The amplifier was then tuned at the desired frequency of operation, 5.0 GHz, for minimum noise by adjusting input inductance and for maximum input return loss by adjustment of first-stage source lead inductance and drain inductance. In this case, the feedback is used to achieve input match, z_{FB} is primarily resistive, and little attention was paid to the gain versus frequency response as the application was narrow band. The resulting gain, noise temperature, and input return loss at 300 K and 20 K are shown in Fig. 16. The results are flawed by the decrease in input return loss at 20 K; this is probably due to the change in g_m effecting z_{FB} . Another version of this amplifier was used with an input cooled isolator to achieve input match and a noise temperature of 17 K at 5.0 GHz.

It is particularly desirable for cryogenic GASFET amplifiers to achieve match by feedback (or perhaps by a

balanced configuration) since ferrite devices usually do not function well at both room and cryogenic temperatures. Our goal has been to construct an amplifier which is wide band, matched, performs well at both room and cryogenic temperatures, and hence does not utilize ferrite isolators. All of the above characteristics have not yet been achieved in a single unit; work will continue in this direction.

VII. CONCLUSIONS

All of the questions posed in the Introduction have not been answered and in some cases the answers are "hints" based on insufficient data; more work, both experimental and theoretical, is needed. Some conclusions that may be ventured are as follows.

A. Thermal Considerations

1) At temperatures above 15 K there is no fundamental problem in the cooling of a FET but attention must be paid to the fact that materials have vastly different thermal conductivity at cryogenic temperatures. In particular alumina, Kovar, and epoxy (whether silver loaded or not) become near insulators.

At temperatures below 15 K the thermal conductivity between the FET channel and the chip is greatly reduced due to boundary scattering of phonons and little can be done to alleviate this problem.

B. DC Characteristics and Material Properties

1) Changes in pinch-off voltage, barrier potential, and linear resistances within FET have been found, experimentally, to be small (see Fig. 3 and Table II) in the range 300 K–20 K. This implies that the changes in carrier density and mobility are small.

2) As the temperature was reduced from 300 K to 20 K, saturation current increased by 30–50 percent for the FET's of three manufacturers (see Fig. 3). This implies that the saturation velocity increases as the device is cooled; the differences between devices are due to either different doping density or some other constituent of the GaAs.

3) For the same 3 devices the output resistance decreased from 30–200 percent upon cooling; this has not been explained.

C. Small-Signal Characteristics

Transconductance increased by the same factor as saturation current and this causes an increase in RF gain that is somewhat smaller due to negative feedback and a concurrent decrease in output resistance. There is little other change in the gain versus frequency characteristic (see Fig. 5).

D. Noise

1) The noise temperature improvement factor for cooling from 300 K to 20 K varies from 3 to 5 for the six types of transistors tested at 5 GHz (see Fig. 9). It is not known

why the improvement factor varies; more detailed investigation is needed of devices with small improvement factors. The variation may be due to the stronger dependence of noise temperature upon the gate-drain noise correlation coefficient C at cryogenic temperatures.

2) The results for one device, the Mitsubishi MGF 1412, correlate fairly well with the noise theory of Pucel *et al.* [28] both at 300 K and 20 K. The noise improvement is due to the reduction in thermal noise of the channel and parasitic resistances and the increase in transconductance. The nonthermal noise power (hot-electron and high-field diffusion noise) may remain constant or increase at cryogenic temperature; the experimental data is of insufficient accuracy and content to make this judgement. A study of noise variation with bias has recently been performed [58] and forms a further test of the theory.

E. Amplifiers

1) An amplifier has been constructed with performance close to that of the best cooled paramps at 5 GHz (see Fig. 15).

2) It appears feasible, at least for narrow-bandwidths (~ 2 percent) at 5 GHz, to design unbalanced amplifiers which are matched by feedback rather than ferrite devices, and operate well at all temperatures from 300 K to 20 K (see Fig. 16).

3) The reliability of amplifiers constructed with the techniques described in Section VI has been excellent. At the time of this writing, 15 of the basic amplifiers have been constructed and subjected to a total of over forty 300 K to 20 K temperature cycles with no failures.

ACKNOWLEDGMENT

The author wishes to thank C. R. Pace for assistance with the construction and measurements, J. Granlund for the solution of the nonlinear differential equation for the forward-biased gate and for finding the transistor equivalent circuit elements from S -parameter measurements, and T. Brookes for several helpful discussions and the program for calculating results of the Pucel *et al.* noise theory. A. R. Kerr suggested the cooled-attenuator noise measurement procedure and the modification of the attenuator contact. The author appreciates the S -parameter measurements performed by R. Hamilton of Avantek, Inc. and R. Lane of California Eastern Laboratories.

REFERENCES

- [1] *Diode and Transistor Designer's Catalog*, Hewlett Packard Co., Palo Alto, CA, 1980.
- [2] *NEC Microwave Transistor Designer's Guide*, California Eastern Laboratories, Santa Clara, CA.
- [3] Data Sheets, LNR Communications, Hauppauge, NY.
- [4] D. M. Burns, "The 600 MHz noise performance of GaAs Mesfet's at room temperature and below," M. S. Thesis, Dep. Elec. Eng., Univ. of California, Berkeley, CA, Dec. 1978.
- [5] D. Williams, S. Weinreb, and W. Lum, "L-band cryogenic GaAs FET amplifier," *Microwave J.*, vol. 23, no. 10, October 1980.
- [6] C. A. Liechti and R. A. Lerrick, "Performance of GaAs MESFET's at low temperatures," *IEEE Trans. Microwave Theory Tech.*, vol. MTT-24, pp. 376-381, 1976.
- [7] J. Pierro and K. Louie, "Low temperature performance of GaAs MESFET's at L-band," 1979 *Int. Microwave Symp. Dig.* (Orlando, FL), IEEE Cat. No. 79CH1439-9, pp. 28-30.
- [8] R. E. Miller, T. G. Phillips, D. E. Iglesias, and R. H. Knerr, "Noise performance of microwave GaAs F.E.T. amplifiers at low temperatures," *Electron. Lett.*, vol. 13, no. 1, pp. 10-11, Jan. 6, 1977.
- [9] J. D. Kraus, *Radio Astronomy*. New York: McGraw Hill, 1966, ch. 7, p. 237.
- [10] Model 21 Cryodyne, CTI-Cryogenics Inc., Waltham, MA, 02154.
- [11] H. F. Cooke, "Fets and bipolars differ when the going gets hot," *Microwaves*, pp. 55-60, Feb. 1978. Also printed as *High-Frequency Transistor Primer, Part III*, Thermal Properties, Avantek Corp., Santa Clara, CA.
- [12] M. G. Holland, "Phonon scattering in semiconductors from thermal conductivity studies," *Phys. Rev.*, vol. 134, pp. A471-480, Apr. 20, 1964.
- [13] *American Institute of Physics Handbook*, 3rd ed. New York: McGraw Hill, 1972.
- [14] *Thermal Conductivity of Solids at Room Temperature and Below*, Monograph 131, National Bureau of Stds, Boulder, CO, Sept. 1973.
- [15] J. Callaway, "Model for lattice conductivity at low temperatures," *Phys. Rev.*, vol. 113, pp. 1046-1051, Feb. 15, 1959.
- [16] C. L. Reynolds and A. C. Anderson, "Thermal conductivity of an electrically conducting epoxy below 3K," *Rev. Sci. Instru.*, vol. 48, no. 12, p. 1715, Dec. 1977.
- [17] C. Kittel, *Introduction to Solid State Physics*, 5th ed. New York: Wiley, 1976.
- [18] H. Fukui, "Determination of the basic device parameters of a GaAs Mesfet," *BSTJ*, vol. 58, no. 3, pp. 771-797, March 1979.
- [19] R. Hackam and P. Harrop, "Electrical properties of nickel-low doped n-type gallium arsenide Schottky barrier diodes," *IEEE Trans. Electron Devices*, vol. ED-19, no. 12, pp. 1231-1238, Dec. 1972.
- [20] D. Vizard, "Cryogenic DC characteristics of millimeter-wavelength Schottky barrier diodes," Appelton Laboratory, Slough, U.K., unpublished.
- [21] F. A. Padovani and R. Stratton, "Field and thermionic-field emission in Schottky barriers," *Solid-State Electron.*, vol. 9, pp. 695-707, 1966.
- [22] T. Viola and R. Mattauch, "High-frequency noise in Schottky barrier diodes," Res. Labs Eng. Sci. Univ. of Virginia, Charlottesville, VA, Rep. EE-4734-101-73J, Mar. 1973.
- [23] M. Giterman, L. Krol, V. Medvedev, M. Orlova, and G. Pado, "Impurity-band conduction in n-GaAs," *Soviet Phys. Solid State*, vol. 4, no. 5, pp. 1017-1018, Nov. 1962.
- [24] O. Emel'yanenko, T. Tagunova, and D. Naselov, "Impurity zones in P- and N-type gallium arsenide crystals," *Soviet Phys. Solid State*, vol. 3, no. 1, pp. 144-147, July 1961.
- [25] P. Wolf, "Microwave properties of Schottky-barrier field-effect transistors," *IBM J. Res. Develop.*, vol. 14, pp. 125-141, Mar. 1970.
- [26] A. Nara, Mitsubishi Semiconductor Laboratory, Hyogo, Japan, private communication.
- [27] J. Ruch and G. Kino, "Transport properties of GaAs," *Phys. Rev.*, vol. 174, no. 3, pp. 921-927, Oct. 15, 1968.
- [28] R. Pucel, H. Haus, and H. Statz, "Signal and noise properties of gallium arsenide microwave field-effect transistors," *Adv. in Electronics and Electron Physics*, vol. 38, L. Morton, Ed. New York: Academic, 1975.
- [29] Model 350 Cryodyne, CTI-Cryogenics, Inc., Waltham, MA.
- [30] A. R. Kerr, Goddard Inst. for Space Studies, New York, NY, private communication.
- [31] Type 2156 Bellows, Servometer Corp., Cedar Grove, NJ.
- [32] Type DT-500-CV-DRC, Lake Shore Cryotronics, Westerville, OH.
- [33] M. Schneider, "Microstrip lines for microwave integrated circuits," *BSTJ* vol. 48, pp. 1421-1444, May 1969.
- [34] T. Suzuki, A. Nara, M. Nakatoni, and T. Ishii, "Highly reliable GaAs MESFET's with a static mean NF_{min} of 0.89 dB and a standard deviation of .07dB at 4 GHz," *IEEE Trans. Microwave Theory Tech.*, vol MTT-27 no. 12, pp. 1070-1074, Dec. 1979.
- [35] Model 75D, Boonton Electronics, Parsippany, NJ.
- [36] R. Lane, California Eastern Laboratories, Santa Clara, CA, private communication.
- [37] R. Hamilton, Avantek Corp., Santa Clara, CA, private communication.

- [38] A. van der Ziel, "Thermal noise in field-effect transistors," *Proc. IRE*, vol. 50, pp. 1808-1812, 1962.
- [39] W. Baechtold, "Noise behavior of GaAs field-effect transistors with short gate lengths," *IEEE Trans. Electron Devices*, vol. ED-19, pp. 674-680, May 1972.
- [40] NE244 Data Sheet, California Eastern Labs, Santa Clara, CA.
- [41] K. Takagi and A. van der Ziel, "High frequency excess noise and flicker noise in GaAs FET's," *Solid-State Electron.*, vol. 22, pp. 285-287, 1979.
- [42] J. Graffeuil, "Static, dynamic, and noise properties of GaAs Mesfets," Ph.D. thesis, Univ. Paul Sabatier, Toulouse, France.
- [43] H. Rothe and W. Dahlke, "Theory of noisy fourpoles," *Proc. IRE*, vol. 44, no. 6, pp. 811-818, June 1956.
- [44] H. Fukui, "Design of microwave GaAs MESFET's for broad-band low-noise amplifiers," *IEEE Trans. Microwave Theory Tech.*, vol. MTT-27, no. 7, pp. 643-650, July 1979.
- [45] Type D-5880 RT/Duroid, .031" dielectric, 1 oz. 2 side copper, Rogers Corp., Chandler, AZ.
- [46] S. Weinreb, M. Balister, S. Maas, and P. J. Napier, "Multiband low-noise receivers for a very large array," *IEEE Trans. Microwave Theory Tech.*, vol. MTT-25, no. 4, pp. 243-248, Apr. 1977.
- [47] Indalloy No. 4 Solder, 100% Indium, 157°C, Indium Corp. of America, Utica, NY.
- [48] #30 Supersafe Flux (water soluble), Superior Flux and Mfg. Co., Cleveland, OH.
- [49] SN62 Solder, 62% Tin, 36% Lead, 2% Silver, 179°C, Multicore Solder, Westbury, NY.
- [50] 20E2 Solder, 100°C, Alpha Metals, Jersey City, NJ.
- [51] #74 Polyester Electrical Tape, 3M Co., Minneapolis, MN.
- [52] L. Nevin and R. Wong, "L-band GaAs FET amplifier," *Microwave J.*, vol. 22, no. 4, p. 82, Apr. 1979.
- [53] J. Frey, "Effects of intervalley scattering on noise in GaAs and InP field effect transistors," *IEEE Trans. Electron Devices*, vol. ED-23, no. 12, pp. 1298-1303, Dec. 1976.
- [54] J. Granlund, "Resistance associated with FET gate metallization," *IEEE Trans. Electron Devices*, to be published.
- [55] N. J. Keen, "The role of the undepleted epitaxial layer in low noise Schottky barrier diodes for millimeter wave mixers," Max-Planck-Institute for Radio Astronomy, Bonn, W. Germany, to be published.
- [56] S. Sesnic and G. Craig, "Thermal effects in JFET and MOSFET devices at cryogenic temperatures," *IEEE Trans. Electron Devices*, vol. ED-19, no. 8, pp. 933-942, Aug. 1972.
- [57] D. Brunet-Brunol, "Etude et réalisation d'amplificateur a transistor a effet de champ a l'GaAs refroidi a très basse température," *Rev. Phys. Appl.*, vol. 13, no. 4, pp. 180-187, Apr. 1978.
- [58] S. Weinreb and T. M. Brookes, "Characteristics of low-noise GaAs MESFET's from 300 K to 20 K," in *Proc. European Microwave Conf.*, 1980.
- [59] COMPACT Network Analysis Program, Compact Engineering Inc., Palo Alto, CA.

Design of Broad-Band GaAs FET Power Amplifiers

CHRISTEN RAUSCHER, MEMBER, IEEE, AND HARRY A. WILLING, MEMBER, IEEE

Abstract—A direct systematic approach to designing broad-band GaAs FET power amplifiers for optimum large-signal gain performance is described. Assets of this approach include its accuracy in predicting large-signal amplifier performance and its basic simplicity. The implementation of the technique is facilitated by having to measure large-signal device behavior at only one single frequency. The practicability of the method is demonstrated through comparisons between measured and predicted results.

I. INTRODUCTION

MICROWAVE GaAs FET's are being used extensively in a wide variety of circuit applications. One of their prominent uses is in large-signal quasi-class-A amplifiers. This paper describes a systematic design procedure for optimizing broad-band gain performance in such amplifiers [1]. Principal assets of the approach are its accuracy in predicting amplifier response at elevated gain compression levels and its simplicity. The simplicity of the method is attributed to the use of a special circuit-type

model to describe large-signal device performance. The principal function of the model is to cast device performance characteristics into an easily manageable format which ultimately permits the nonlinear circuit design problem to be solved efficiently with existing linear synthesis techniques. The derivation of the model proves to be remarkably simple by itself, based solely on large-signal device information obtained experimentally at a single reference frequency. Important to the practical significance of the method is, of course, that its underlying simplicity not stand in the way of accurately predicting large-signal amplifier performance. This is accomplished by focusing on the device nonlinearities that control power gain behavior, and by limiting design considerations to amplifier performance at a designated fixed output power level specified by the particular application.

II. THE METHOD

A. Basic Design Philosophy

The design objective is to achieve maximum flat gain across the frequency band of interest with the transistor

Manuscript received April 30, 1980; revised June 26, 1980.

The authors are with Naval Research Laboratory, Code 6851, Washington, DC 20375.